Meteorological buoy observations from the central Iceland Sea

B. E. Harden[1], I. A Renfrew[2], and G. N. Petersen[3]

[1] Department of Physical Oceanography, Woods Hole Oceanographic Institution, Woods Hole, Massachusetts, USA, [2] School of Environmental Sciences, University of East Anglia, Norwich, UK, [3] Icelandic Meteorological Office, Reykjavik, Iceland

Abstract We present the first continuous in situ atmospheric observations from the central Iceland Sea collected from a meteorological buoy deployed for a 2 year period between 23 November 2007 and 21 August 2009. We use these observations to evaluate the ERA-Interim reanalysis product and demonstrate that it represented low-level meteorological fields and surface turbulent fluxes in this region very well. The buoy observations showed that moderate to strong winds were common from any direction, while wind speeds below 5 ms^{-1} were relatively rare. The observed low-level air temperature and surface heat fluxes were related to the wind direction with cold-air outbreaks most common from the northwest. Mean wintertime turbulent heat fluxes were modest (<60 Wm^{-2}), but the range was substantial. High heat flux events, greater than 200 Wm^{-2}, typically occurred every 1–2 weeks in the winter, with each event lasting on average 2.5 days with an average total turbulent heat flux of ~200 Wm^{-2} out of the ocean. The most pronounced high heat flux events over the central Iceland Sea were associated with cold-air outbreaks from the north and west forced by a deep Lofoten Low over the Norwegian Sea.

1. Introduction

In terms of its physical oceanography and meteorology the Iceland Sea is arguably the least studied of the North Atlantic's subpolar seas. Major field campaigns in the Greenland Sea [e.g., *Schlosser et al.*, 1991; *Watson et al.*, 1999; *Brümmer*, 1997], the Labrador Sea [e.g., *The Lab Sea Group*, 1998; *Renfrew et al.*, 1999], and the Irminger Sea and Denmark Strait [e.g., *Pickart et al.*, 2003; *Renfrew et al.*, 2008] have given a picture of the dense water production in these regions and the role of air-sea fluxes in driving this process. As the most accessible, and motivated by operational weather forecasting, the Norwegian Sea has generally received consistent attention. In contrast, the Iceland Sea—between Iceland and Jan Mayen (see Figure 1)—has generally garnered less scientific attention.

This is now changing, in part because of the discovery of the North Icelandic Jet [*Jónsson and Valdimarsson*, 2004], a new pathway of dense water that flows along the north slope of Iceland and feeds the Denmark Strait Overflow, a major source of the Deep Western Boundary Current. The North Icelandic Jet is thought to transport southward up to half of Denmark Strait's dense water [*Våge et al.*, 2011] and is hypothesized to originate in the Iceland Sea [*Våge et al.*, 2013]. However, its exact source and related water mass transformation processes are currently unknown. Deep convection in the Iceland Sea had been previously discussed by *Swift and Aagaard* [1981], but it is the new potential role that the Iceland Sea plays in feeding the Denmark Strait Overflow that focuses our attention on where and when deep convection could occur, and the atmospheric conditions and surface heat fluxes that might drive it.

From a meteorological standpoint, what is maybe most perplexing about the prospect of dense water formation in the Iceland Sea is that this region is a local heat flux minimum [*Moore et al.*, 2012]. In other regions of oceanic deep convection, for example, the Labrador Sea, Greenland Sea, and the Irminger Sea, the large-scale atmospheric circulation ensures consistently high heat fluxes and, as such, readily promotes water mass transformation. However, in the Iceland Sea, *Moore et al.* [2012] show that the Iceland Sea is at a saddle point between the climatological Icelandic and Lofoten Lows, and according to ERA-Interim reanalyses, the winter-mean heat fluxes are only 57 Wm^{-2} (out of the ocean), with winter-mean air and sea surface temperatures of 1.3 and 2.3°C, respectively. Using composites of high and low heat flux months, they show that this local minimum is the result of a balance between relatively low heat flux months (including negative heat fluxes—the atmosphere warming the ocean) and modest heat flux months; e.g., the average of the highest 10% of months has a total surface heat flux of 116 Wm^{-2}. It is unlikely that such modest heat fluxes would be sufficient to drive deep convection in the Iceland Sea even during high heat flux months.
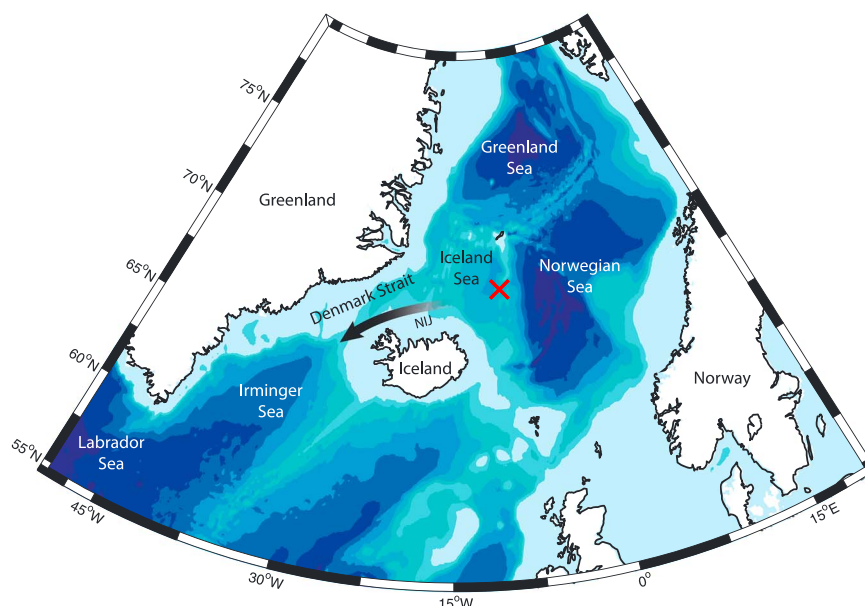
Figure 1. Map showing key locations and features referred to in the text. The location of the meteorological buoy in the Iceland Sea is shown with a red cross. The bathymetry is plotted every 500 m. The North Icelandic Jet (NIJ) is shown along the north slope of Iceland. This newly discovered current is thought to originate in the Iceland Sea and feed the Denmark Strait with half its dense overflow water.

However, *Moore et al.* [2012] only used monthly mean fields and were not able to detail the characteristics of typical air-sea flux events. It is clear that we need to increase our temporal resolution if we are to determine, for example, whether the surface fluxes in the highest heat flux months are consistently moderate (around 100 Wm^{-2} of cooling) or are composed of episodic periods of higher and lower heat fluxes as is prevalent in the Labrador Sea [*Renfrew et al.*, 2002] and Irminger Sea [*Våge et al.*, 2008]. Moreover, we do not currently know whether there are locations in the Iceland Sea that might be susceptible to stronger forcing than the basin-scale mean. This knowledge would be vital to inform deep convection studies and focus field campaigns in the region.

Moore et al. [2012] also did not establish how close the reanalysis flux fields are to observations in the Iceland Sea. Reanalyses are powerful tools for investigating air-sea interaction, but only if we can validate their low-level fields. Calculating turbulent heat fluxes in reanalyses is sensitive to the representation of sea surface temperature, low-level properties, and stability [*Renfrew et al.*, 2002], and validating these fields is hard in regions with sparse in situ observations, such as the Nordic Seas. Reanalyses have been shown to exhibit both low and high heat flux biases in other regions of the subpolar and polar seas [*Lammert et al.*, 2010; *Harden et al.*, 2011; *Jakobson et al.*, 2012] highlighting the importance of local verification of heat flux products, especially in the Iceland Sea which sits at a large-scale confluence of diverse air masses.

The aim of this paper is to address some of these knowledge gaps and provide a more in-depth look at the temporal and spatial scales of air-sea fluxes in the Iceland Sea. To do this, we use in situ observations from a meteorological buoy deployed in the central Iceland Sea for almost 2 years. We use this data to present a brief surface climatology and provide valuable validation for a global reanalysis product (ERA-Interim). We then use the buoy observations, in conjunction with reanalyses fields, to determine the atmospheric forcing one might expect for different synoptic-scale situations and to characterize the temporal and spatial extent of high heat flux events.

2. Data

The meteorological buoy was deployed by the Icelandic Meteorological Office in the central Iceland Sea to obtain information on local weather as a part of a governmental preparation phase for exploration for oil and gas on the Icelandic continental shelf. The buoy was deployed from 23 November 2007 to 21 August 2009 and was anchored at 68.47°N, 9.27°W (see Figure 1 for location). It was serviced once during this period on 7 June 2008. The buoy measured wind velocity (at a height of 4 m), air temperature (3.5 m), humidity (3.5 m), and

sea level pressure with a time resolution of 1 h. In addition, the buoy measured the ocean temperature and velocity at 1.5 m depth. The meteorological data were adjusted to standard heights using well-established stability-dependent formulas, based the algorithm of *Smith* [1988], with constant exchange coefficients from *DeCosmo et al.* [1996], with the same algorithms also used to calculate bulk fluxes. The sea surface temperature needed for this was available from the buoy. This method has previously been shown to be reasonably accurate for the subpolar seas [e.g., *Renfrew et al.*, 2009]. All data were quality controlled manually by removing outliers and other nonphysical data points. The pressure sensor suffered some water damage after two large storms; times when this was clearly a problem have been removed from the analysis.

After 17 April 2009, the buoy broke free of its mooring and drifted northward in the Iceland Sea. It was later recovered on 21 August 2009 at 69.40°N, 9.62°W. During this period the buoy recorded no ocean properties, but the collection of meteorological data was unaffected and the buoy stayed mostly within the same ERA-Interim grid box. To produce a continuous time series of observed surface heat fluxes and to implement the stability-dependent height adjustments at these times, we used the reanalysis sea surface temperature which, as we will show, agrees well with the observations (Figure 2).

We will use the buoy data to validate the European Centre for Medium-Range Weather Forecasts (ECMWF)'s ERA-Interim reanalysis product [*Berrisford et al.*, 2009] for the central Iceland Sea region. This product is a 6-hourly consistent analysis of the atmospheric conditions produced by constraining a global forecast model to observations using a 4D-VAR data assimilation system [*Berrisford et al.*, 2009; *Dee et al.*, 2011]. ERA-Interim has 255 horizontal spectral modes (T255) and 60 vertical levels. For grid point fields, a reduced Gaussian grid is used with an approximate spacing of 80 km. For near-surface variables we use the analysis output every 6 h interpolated onto a uniform latitude-longitude grid of 0.70°. Comparisons with buoy data are made for the nearest grid point in the ERA-Interim product. Sensitivity tests with surrounding grid points showed that the nearest grid point has the best comparison, but the sensitivity in this central Iceland Sea location is not large.

The surface turbulent fluxes that are available from ERA-Interim are diagnostic quantities accumulated over 3 h intervals from a forecast. We use the output on the same 6-hourly temporal resolution as the analysis fields. This means that, for example, the 00 UTC fluxes that we present are actually an average over the 3 h from 00 to 03 UTC and the 06 UTC fluxes are an average over the 3 h from 06 to 09 UTC. We use a similar 3 h averaging of the buoy fluxes to enable a direct comparison to the ERA-Interim flux data.

3. Results

3.1. Reanalysis Verification

In general, the ERA-Interim reanalyses compare remarkably well with the buoy observations (Table 1 and Figure 2). The correlation coefficients are high, the linear regression slopes are close to unity, and the bias errors are relatively small. Perhaps the most notable bias is 0.43°C in the 2 m air temperature (T_{2m}), which combined with a -0.34°C bias in SST means a bias in the air-sea temperature difference of almost 0.8°C. The modeled relative humidity has a moderate spread and a bias of -5.5%, although this only equates to a small bias in specific humidity. Root-mean-square errors in the turbulent heat fluxes are both around 15 Wm^{-2}, and the biases are relatively small and negative. ERA-Interim underestimates the heat leaving the ocean, mostly due to the 2 m air and sea surface temperature biases noted above.

ERA-Interim is biased marginally high for wind speed (by 0.12 ms^{-1}) compared to the Iceland Sea buoy observations. This is unusual compared to previous such comparisons in the region, which typically show that reanalyses underestimate wind speeds [e.g., *Renfrew et al.*, 2002; *Moore et al.*, 2008; *Renfrew et al.*, 2009; *Harden et al.*, 2011]. To investigate this further, we conditionally sampled for wind direction and found that the bias was significantly greater for southerlies (0.39 ms^{-1} or 5.2% of the southerly mean) than it was for northerlies (-0.09 ms^{-1} or 1.1% of the northerly mean). We hypothesize that this bias is due to ERA-Interim's poor representation of the sheltering effect of Iceland. The topography of Iceland is known to generate significant jets and wakes [*Smith*, 1982; *Renfrew et al.*, 2008]; during southerly flows a wake region commonly occurs in the lee of Iceland (to the north) and this can extend into the central Iceland Sea. We suggest that a poor representation of this wake in ERA-Interim, due to the model's relatively coarse resolution, could be the cause of this wind bias. Another cause of the bias for southerly flow might be how ERA-Interim represents low-level, stable boundary conditions that might be formed when warm air from the south is advected over the relatively cold
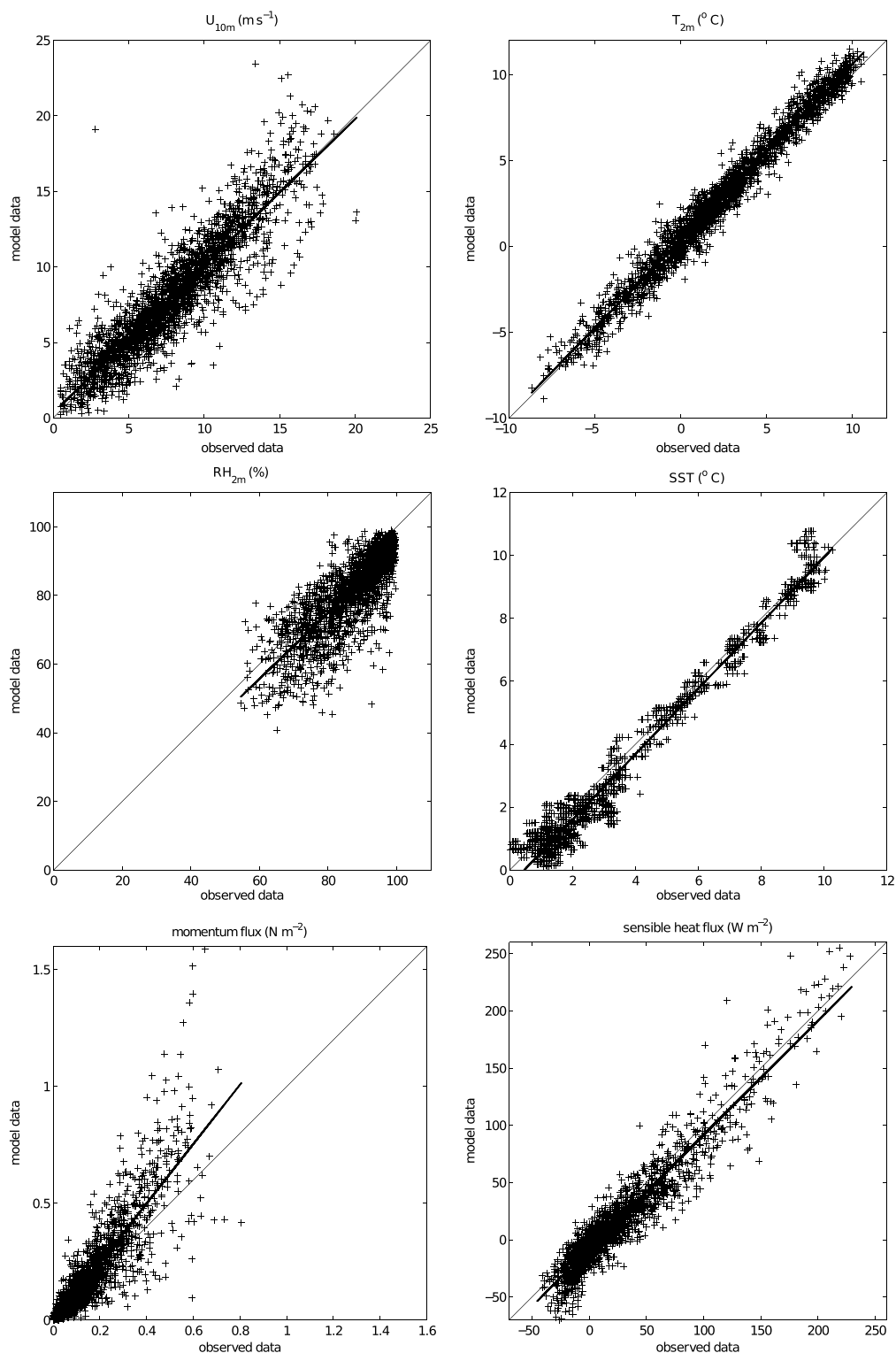
Figure 2. Meteorological buoy observations versus ERA-Interim reanalyses values as scatterplots for the ~2 year deployment. Panels are the 10 m wind speed (U_{10m}), 2 m air temperature (T_{2m}), 2 m relative humidity (RH_{2m}), sea surface temperature (SST), surface momentum flux, and surface sensible heat flux. A linear regression line is overlaid (bold).

Table 1. Comparison of ERA-Interim With Meteorological Buoy Data[a]

	MSLP (hPa)	T_{2m} (°C)	SST (°C)	q_{2m} (gkg^{-1})	RH$_{2m}$ (%)	U_{10m} (ms^{-1})	WD (deg)	τ (Nm^{-2})	SHF (Wm^{-2})	LHF (Wm^{-2})
Mean: buoy	1004.7	2.39	3.45	4.18	88.3	7.91	162	0.131	20.5	34.0
ERA-Interim	1004.9	2.82	3.11	4.09	82.8	8.03	157	0.158	12.3	27.6
SD: buoy	14.1	3.93	2.72	1.40	9.7	3.62	107	0.127	39.9	38.6
ERA-Interim	14.0	4.08	2.88	1.48	11.3	3.88	105	0.183	42.1	38.6
Correlation coefficient	0.99	0.99	0.99	0.98	0.83	0.91	0.97	0.89	0.95	0.94
Slope	0.99	1.02	1.04	1.04	0.96	0.97	0.98	1.27	1.00	0.95
Bias error	0.12	0.43	−0.34	−0.09	−5.5	0.12	−5	0.026	−8.3	−6.4
RMS error	0.54	0.82	0.61	0.30	8.4	1.6	23	0.095	15.8	14.4
Number	920	2536	2029	2439	2439	2536	2415	2536	2536	2439

[a]Comparison of 6-hourly buoy observations and ECMWF Interim reanalysis time series for mean sea level pressure, MSLP (hPa); 2 m temperature, T_{2m} (°C); sea surface temperature, SST (°C); 2 m specific humidity, q_{2m} (gkg^{-1}); 2 m relative humidity, RH$_{2m}$ (%); wind speed, U_{10m} (ms^{-1}); wind direction, WD (deg); surface momentum flux, τ (Nm^{-2}); surface sensible heat flux, SHF (Wm^{-2}); and surface latent heat flux, LHF (Wm^{-2}). The number of points used in the comparisons is shown in the last row. Note that to avoid spurious wind direction statistics if the difference in wind direction is greater than 270°, it is assumed that this is because of a 360-0 crossing and these points are neglected.

ocean in the Iceland Sea. Resolving wakes and boundary layers accurately could therefore be important for representing wind strength and air masses over the Iceland Sea and improving air-sea fluxes.

However, there are other possibilities for the wind speed bias. Previous studies have shown that sheltering effects and elevation changes during rough seas can negatively bias the wind field measured by met buoys at high wind speeds [*Large et al.*, 1995; *Zeng and Brown*, 1998]. In addition, the met buoy measures flow features on a smaller spatial scale than ERA-Interim; there is a representativity uncertainty due this point measurement being compared to a grid box average, possibly leading to the buoy recording higher winds than ERA-Interim, as discussed by, e.g., *Stoffelen* [1998]. However, this representativity uncertainty does not explain the inconsistency of our comparison with previous comparisons for the subpolar seas [e.g., *Renfrew et al.*, 2002; *Moore et al.*, 2008; *Renfrew et al.*, 2009; *Harden et al.*, 2011].

Our comparison for the central Iceland Sea is noticeably better than previous studies in other subpolar seas. *Renfrew et al.* [2009] compared aircraft-based observations for the Irminger Sea, Denmark Strait, and one flight over the Iceland Sea, to two resolutions of ECMWF operational analyses. That version of the ECMWF forecast system was very similar to that employed for ERA-Interim. In our comparison the wind speed slope, bias, and RMS errors are significantly improved (slope is 0.97 here compared to 0.73 in *Renfrew et al.* [2009]; and the RMS error is 1.6 ms^{-1} compared to 2.6 ms^{-1} in *Renfrew et al.* [2009]); the temperature comparison is better ($r = 0.99$, compared to 0.92 in *Renfrew et al.* [2009]); and the humidity comparison is similar. These differences may be partly explained by the persistent strong wind, cold air outbreak conditions in the *Renfrew et al.* [2009] comparison, which produced large errors over, and downwind, of the sea ice zone.

One can also compare the performance of ERA-Interim in our study to that of the North American Regional Reanalyses (see *Mesinger et al.* [2006]) when compared to a meteorological buoy in the Irminger Sea—see *Moore et al.* [2008]. Here despite a coarser horizontal resolution, the ERA-Interim generally performs better; e.g., T_{2m}, U_{10m}, and humidity are all better represented. In addition, in the nearby Denmark Strait and northern Irminger Sea, *Harden et al.* [2011] showed that the 2 m air temperature in ERA-Interim is negatively biased by −1°C resulting in surface fluxes being too large by ∼10%. We have shown that this is not the case in the central Iceland Sea; ERA-Interim is marginally high biased in its 2 m temperature and slightly underestimates heat fluxes. Even though we are only just upstream of their study region, this comparison demonstrates the need for local verification of reanalyses, especially over the subpolar seas that experience a wide range of wind regimes.

3.2. Wind Field

The Iceland Sea sits at a saddle point between the competing influences of the Icelandic Low to the west and the Lofoten Low to the east [*Moore et al.*, 2012]. The result is that, although the mean wind field is weakly from
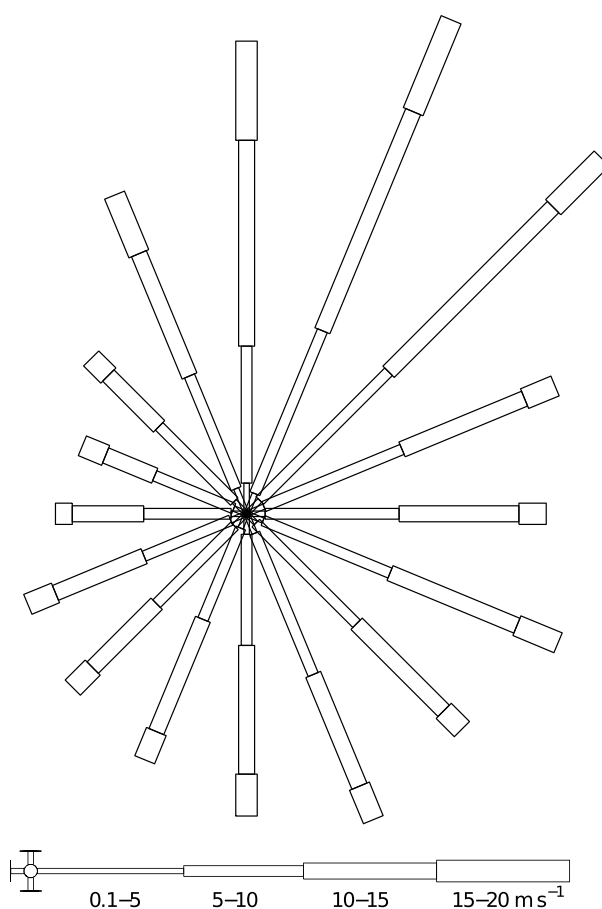
Figure 3. Wind rose for the central Iceland Sea based on observed 10 m winds from the meteorological buoy. The wind direction is divided into 22.5° bins (i.e., N, NNE, NE, etc.) and the wind speed into 5 ms^{-1} bins. The width of the bar is proportional to the wind speed, and the length is proportional to the frequency from that direction.

the northeast, the instantaneous wind field is typically moderate to strong (10–20 ms^{-1}) and from a range of directions (Figure 3). Winds from all directions are common, with a slight preference toward northeasterly flow and fewer occurrences of westerly flow. It is very rare for the winds to be lower than 5 ms^{-1}.

In order to more fully describe the low-level wind field we employed a detection routine to find high wind speed events. In light of the lack of a well-defined preferred wind direction, we employed this detection routine for all wind directions in 15° increments. We resolved the wind velocity into each direction, then found all of the local maxima greater than a threshold of 10 ms^{-1}, and separated by more than 48 h (to allow time between synoptic systems). If two maxima were found to be closer than 48 h, then the larger of the two events was chosen. The following results are qualitatively similar for different choices of wind speed threshold or event spacing.

For each event, from each direction, we calculate the mean 2 m temperature and total turbulent heat flux as measured by the met buoy in a 12 h window centered on the wind event. In addition, we used the low-level fields from ERA-Interim at the nearest model time step to represent the wide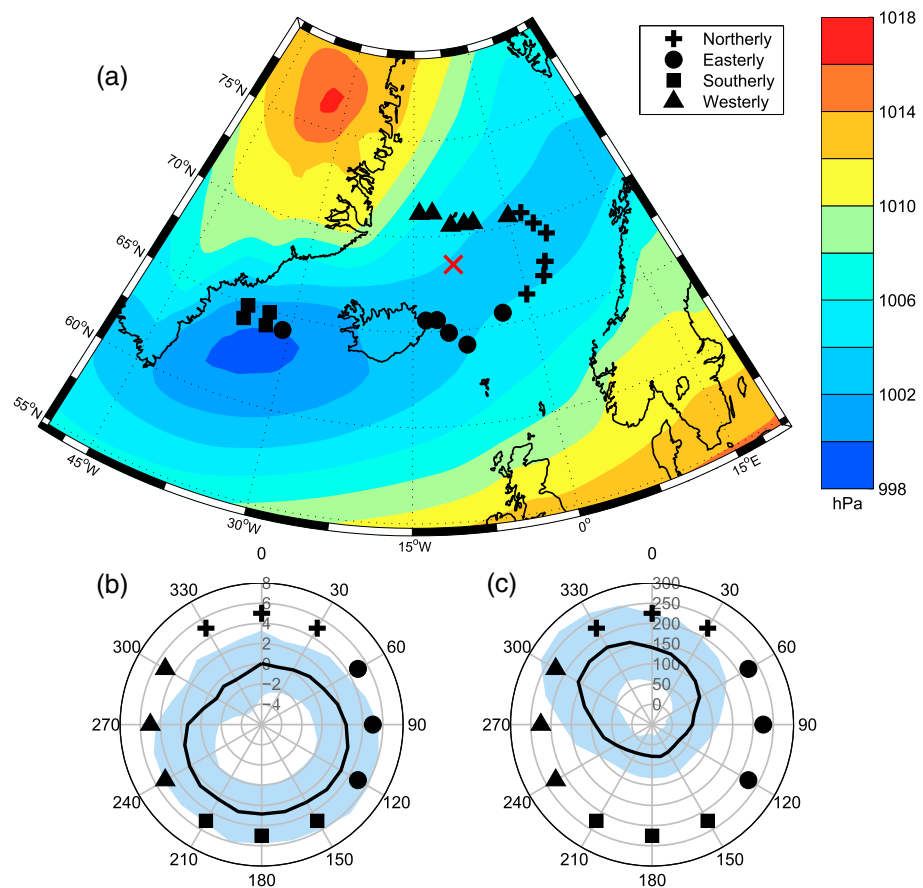r meteorological environment at the time of the event. The number of wind events is not equally distributed through the range of directions. In accordance with the wind rose (Figure 3), the largest number of events are found for northerly flow (68 events), and the fewest for westerly flow (31 events). Most events are triggered between the months of September and May.

Each high wind speed event was triggered by a passing low-pressure system (as seen from manually inspecting individual events, not shown). For each wind direction, we produced a composite pressure field from the ERA-Interim data as a mean over all the events. This allowed us to map the centers of action and determine where a typical storm that triggers a high wind event from a given angle resides. The location of the low pressure center at the time of the wind maximum determines the wind direction at the buoy site (Figure 4). For example, lows over the Norwegian Sea will trigger northerly wind events, while lows along the southeast coast of Greenland will trigger southerly wind events. The Norwegian and Irminger Seas are both regions of seasonally lower pressure where more storms pass during the winter. As such, a higher proportion of winds come from these directions (Figure 3). To trigger a westerly event, the pressure center has to be confined close to the east coast of Greenland, where lows are less frequently found, hence the fewer events and the weaker mean winds from this direction.

For a given high wind speed event direction the synoptic-scale pressure system will draw in air with markedly different properties (Figure 4). At the most extreme, northwesterly events draw in cold, dry Arctic air off the sea ice to the north and west. Air temperatures are on average −1°C (±1 standard deviation of +3 to −5°C) but can be as low as −9°C during these events. In contrast, southeasterly events bring in warm maritime air that is on average 3°C but can be as warm as 10°C in extreme cases. Accompanying these shifts in temperature are

Figure 4. The influence of the synoptic scale situation on temperature and heat fluxes at the meteorological buoy (the red cross in Figure 4a). (a) The location of the center of composite low-pressure systems (shaped markers) as a function of wind direction at the buoy (in 15° increments, see text), grouped into four predominant directions: northerly winds (pluses, 315°–30°), easterly winds (circles, 45°–120°), southerly winds (squares, 135°–210°), and westerly winds (triangles, 225°–300°). There are six low centers for each wind direction group. For southerly events, the ERA-Interim horizontal resolution means that multiple low pressure centers fall on the same grid point, hence the few number of markers for this direction group. Shaded contours show the wintertime (October to April) mean sea level pressure field from ERA-Interim for the 2 years of deployment. (b and c) Polar plots of the range in mean 2 m air temperature (°C) and mean total turbulent heat flux (Wm^{-2}), respectively, measured by the buoy over a 12 h window centered on the events from each wind direction. The mean (bold line) and ±1 standard deviation (light blue shading) are plotted. Gray axial lines and shaped markers are plotted for every second wind direction used in the analysis.

large changes in total surface heat flux over the Iceland Sea. The cold, dry air of the northwesterly events draws on average more than 150 Wm^{-2} from the ocean, although in some events the heat flux exceeds 300 Wm^{-2}. On the other hand, the southwesterly events produce little to no heat flux due to their high temperatures and humidity.

3.3. Heat Fluxes

In the mean, the heat flux field over the Iceland Sea is a local minimum [*Moore et al.*, 2012]. However, the time series of heat fluxes from the met buoy (Figure 5) clearly shows that isolated high heat flux events can occur on short time scales. The probability distribution is centered near to zero but has a very long tail; the 95th percentile is 211 Wm^{-2} and the 99th percentile is 336 Wm^{-2}. This latter value is low compared to the ~1000 Wm^{-2} reported by *Gulev and Belyaev* [2012] for the 99th percentile in this region based on the National Centers for Environmental Prediction (NCEP) reanalyses fluxes. Even given the moderate high bias of NCEP fluxes at large values [*Renfrew et al.*, 2002; *Moore and Renfrew*, 2002] this is a large discrepancy. Part of this could result from the coarser resolution of the NCEP reanalysis or the limited period of our data (2 years) compared to that used by *Gulev and Belyaev* [2012] (60 years), allowing them to sample more extreme events.
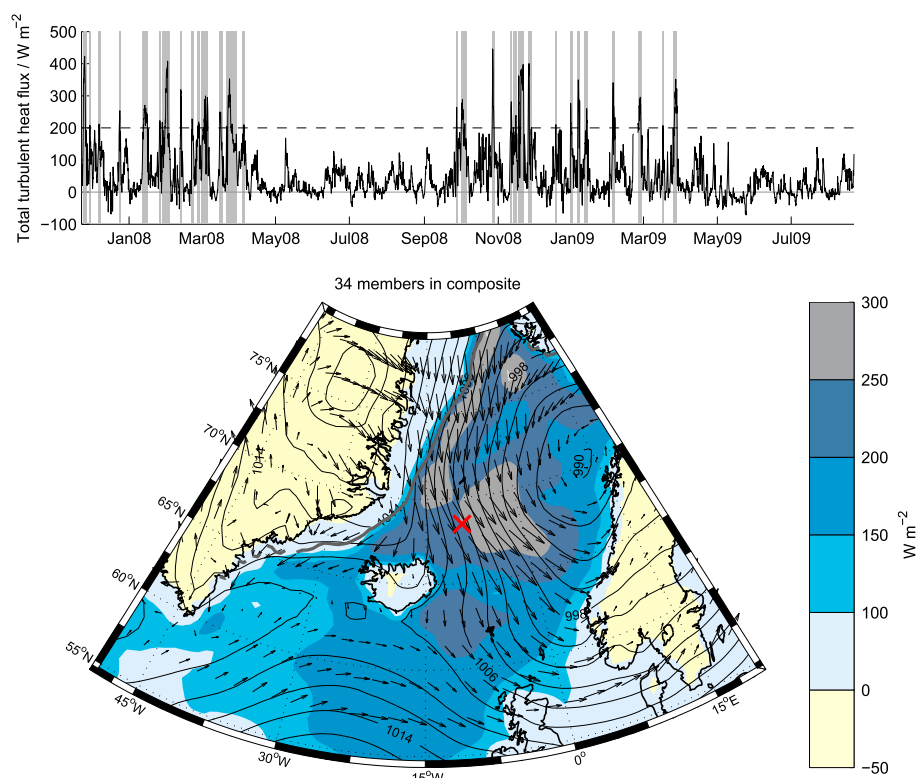
Figure 5. (top) Time series of total turbulent heat flux calculated from the buoy observations, grey bars indicate high heat flux events (see text for details). (bottom) Composite of total turbulent heat flux (shading), mean sea level pressure (contours every 2 hPa) and 10 m winds (vectors) for all of the high heat flux events. The location of the meteorological buoy is marked with a red cross. The mean wintertime sea ice edge is shown with a thick gray line.

To examine high heat flux events in more detail, we applied a similar detection routine to that for the high wind speed events. High heat flux events are defined as peaks in the total turbulent heat flux of over 200 Wm^{-2}, separated by at least 48 h with a minimum of less than 100 Wm^{-2} between peaks to ensure distinct events are being sampled. We chose 200 Wm^{-2} as our threshold as this corresponds to approximately the 95th percentile of heat fluxes. Higher values produce qualitatively similar results but reduce the number of events that are afforded for statistics and compositing. We defined the length of an event as the time that the heat flux was greater than 100 Wm^{-2}. In this manner, we found 34 high heat flux events in the buoy time series.

All the events are clustered in the winter months, between October and April (Figure 5). On average, events lasted 2.5 days (with a standard deviation of 1.5 days) and the longest event lasted 7 days. Over the duration of each event, the mean total turbulent heat flux was 199 Wm^{-2} with the largest event extracting an average of 299 Wm^{-2} over a 3.5 day period. Between events the heat fluxes are relatively small (e.g., see Figures 4 and 5) with 43% of measured total heat fluxes below 20 Wm^{-2}. The result is a moderate record-long mean of 54.5 Wm^{-2} (Table 1). Consequently, the designation of the Iceland Sea as a local minimum disguises the impact of individual high heat flux events.

The meteorological conditions during these high flux events are characteristic of cold-air outbreaks (Figure 5). A strong composite Lofoten Low is over the eastern Norwegian Sea, which drives strong northerly winds, bringing cold, dry air off the ice and over the Iceland Sea. Although these events are representative of local heat flux maxima at the buoy location, higher heat fluxes elsewhere in the region are possible during these events. Of particular interest is the region of high heat flux to the northwest of the buoy location along the ice edge. Here the ocean is likely to experience the coldest, driest air and hence the largest heat fluxes. We speculate that this region could be particularly important for forcing deep convection in the Iceland Sea although the use of the ERA-Interim, or other reanalyses or model fluxes, at this transition needs to be verified observationally.

Our analysis shows that isolated high heat flux events occur in the Iceland Sea and that these events are disguised in annual and monthly means by low fluxes between them. However, the heat fluxes we report during events are modest ($\sim$200 Wm^{-2}) in contrast to events in other regions of deep convection such as the Labrador Sea and Greenland Sea ($\sim$500–1000 Wm^{-2} [*The Lab Sea Group*, 1998; *Watson et al.*, 1999]). As we have discussed, it might be possible for areas near the ice edge to experience larger fluxes, but it remains to be seen whether these are supported by observations and whether they are large enough to drive the water mass conversions that are hypothesized to be occurring in the Iceland Sea.

4. Discussion and Conclusions

We have examined the surface meteorological conditions in the central Iceland Sea from 2 years of observations from a meteorological buoy and the ERA-Interim reanalysis product. In general, ERA-Interim appears to be doing a very good job at representing the low-level meteorological conditions in the central Iceland Sea. The low-level temperature biases witnessed in previous work for the Denmark Strait (low) and in the Arctic (high) are largely absent in this region, and as a result, the turbulent heat fluxes are well represented. The 10 m wind is slightly biased high in the ERA-Interim, during high wind speeds from the south, potentially due to the poor model representation of wake effects in the lee of Iceland.

A wide range of possible storm positions relative to the Iceland Sea ensures that a range of wind directions occur, with a slight preference toward northeasterly flow and fewer westerlies. The wind speed is rarely below 5 ms^{-1}. Thus, the Iceland Sea can be characterized as a part of the North Atlantic that is always experiencing moderate to strong winds with the wind direction changing on synoptic time scales. The different wind directions bring with them air masses from very different sources. At the extremes, northwesterlies bring cold, dry air down from the Arctic and southeasterlies bring warmer, moist air from southern latitudes. These regimes change on synoptic timescales resulting in a rapidly changing turbulent heat flux field over the Iceland Sea. This, coupled to generally cooler ocean temperatures in the region, means that the mean turbulent heat flux is a local minimum for the subpolar North Atlantic. Other regions either have higher surface temperatures or experience more consistent cool, dry conditions.

However, on shorter timescales the Iceland Sea frequently experiences high heat flux events in the wintertime. We find 34 high heat flux events over the two winters, i.e., an event every week or so. Each event lasted on average 2.5 days, extracting on average 199 Wm^{-2} from the ocean. These events occurred during cold-air outbreaks driven by low pressure centers over the Norwegian Sea (i.e., a deep Lofoten Low). At these times, the largest heat fluxes were found nearest to the ice edge, to the north of the buoy, due to the large temperature difference found here. However, given the distance of the ice edge from the buoy, additional in situ observations are needed to verify reanalyses products in this area. Between high heat flux events, the overlying atmosphere was typically moist and at a similar temperature to the ocean ensuring near-zero surface heat fluxes.

References

Berrisford, P., K. D. Dee, M. Fielding, P. Fuentes, S. K. Kallberg, and S. Uppala (2009), ERA report series: 1. The ERA-Interim archive, *Tech. Rep.* European Centre for Medium-Range Weather Forecasts, Reading, U. K.

Brümmer, B. (1997), Boundary layer mass, water, and heat budgets in wintertime cold-air outbreaks from the Arctic sea ice, *Mon. Weather Rev.*, 125(8), 1824–1837, doi:10.1175/1520-0493(1997)125<1824:BLMWAH>2.0.CO;2.

DeCosmo, J., K. B. Katsaros, S. D. Smith, R. J. Anderson, W. A. Oost, K. Bumke, and H. Chadwick (1996), Air-sea exchange of water vapor and sensible heat: The Humidity Exchange Over the Sea (HEXOS) results, *J. Geophys. Res.*, 10(C5), 12,001–12,016, doi:10.1029/95JC03796.

Dee, D. P., et al. (2011), The ERA-Interim reanalysis: Configuration and performance of the data assimilation system, *Q. J. R. Meteorol. Soc.*, 137(656), 553–597, doi:10.1002/qj.828.

Gulev, S. K., and K. Belyaev (2012), Probability distribution characteristics for surface air–sea turbulent heat fluxes over the global ocean, *J. Clim.*, 25(1), 184–206, doi:10.1175/2011JCLI4211.1.

Harden, B. E., I. A. Renfrew, and G. N. Petersen (2011), A climatology of wintertime barrier winds off southeast Greenland, *J. Clim.*, 24(17), 4701–4717, doi:10.1175/2011JCLI4113.1.

Jakobson, E., T. Vihma, T. Palo, L. Jakobson, H. Keernik, and J. Jaagus (2012), Validation of atmospheric reanalyses over the central Arctic Ocean, *Geophys. Res. Lett.*, 39, L10802, doi:10.1029/2012GL051591.

Jónsson, S., and H. Valdimarsson (2004), A new path for the Denmark Strait overflow water from the Iceland Sea to Denmark Strait, *Geophys. Res. Lett.*, 31, L03305, doi:10.1029/2003GL019214.

Lammert, A., B. Brümmer, M. Haller, G. Müller, and H. Schyberg (2010), Comparison of three weather prediction models with buoy and aircraft measurements under cyclone conditions in Fram Strait, *Tellus A*, 62(4), 361–376, doi:10.1111/j.1600-0870.2010.00460.x.

Large, W. G., J. Morzel, and G. B. Crawford (1995), Accounting for surface wave distortion of the marine wind profile in low-level ocean storms wind measurements, *J. Phys. Oceanogr.*, 25(11), 2959–2971, doi:10.1175/1520-0485(1995)025<2959:AFSWDO>2.0.CO;2.

Mesinger, F., et al. (2006), North American regional reanalysis, *Bull. Am. Meteorol. Soc.*, 87(3), 343–360, doi:10.1175/BAMS-87-3-343.

Moore, G. W. K., and I. A. Renfrew (2002), An assessment of the surface turbulent heat fluxes from the NCEP–NCAR reanalysis over the Western Boundary currents, *J. Clim.*, *15*(15), 2020–2037.

Moore, G. W. K., R. S. Pickart, and I. A. Renfrew (2008), Buoy observations from the windiest location in the world ocean, Cape Farewell, Greenland, *Geophys. Res. Lett.*, *35*, L18802, doi:10.1029/2008GL034845.

Moore, G. W. K., I. A. Renfrew, and R. S. Pickart (2012), Spatial distribution of air-sea heat fluxes over the sub-polar north Atlantic Ocean, *Geophys. Res. Lett.*, *39*, L18806, doi:10.1029/2012GL053097.

Pickart, R. S., M. A. Spall, M. H. Ribergaard, G. W. K. Moore, and R. F. Milliff (2003), Deep convection in the Irminger Sea forced by the Greenland tip jet, *Nature*, *424*(6945), 152–156, doi:10.1038/nature01729.

Renfrew, I. A., G. W. K. Moore, T. R. Holt, S. W. Chang, and P. Guest (1999), Mesoscale forecasting during a field program: Meteorological support of the Labrador Sea deep convection experiment, *Bull. Am. Meteorol. Soc.*, *80*(4), 605–620, doi:10.1175/1520-0477(1999)080<0605:MFDAFP>2.0.CO;2.

Renfrew, I. A., G. W. K. Moore, P. S. Guest, and K. Bumke (2002), A comparison of surface layer and surface turbulent flux observations over the Labrador Sea with ECMWF analyses and NCEP reanalyses, *J. Phys. Oceanogr.*, *32*(2), 383–400, doi:10.1175/1520-0485(2002)032<0383:ACOSLA>2.0.CO;2.

Renfrew, I. A., et al. (2008), The Greenland flow distortion experiment, *Bull. Am. Meteorol. Soc.*, *89*(9), 1307–1324, doi:10.1175/2008BAMS2508.1.

Renfrew, I. A., G. N. Petersen, D. Sproson, G. W. K. Moore, S. Adiwidjaja, H. Zhang, and R. North (2009), A comparison of aircraft-based surface-layer observations over Denmark Strait and the Irminger Sea with meteorological analyses and QuikSCAT winds, *Q. J. R. Meteorol. Soc.*, *135*(2046), 2046–2066, doi:10.1002/qj.444.

Schlosser, P., G. Bönisch, M. Rhein, and R. Bayer (1991), Reduction of deepwater formation in the Greenland Sea during the 1980s: Evidence from tracer data, *Science*, *251*(4997), 1054–1056, doi:10.1126/science.251.4997.1054.

Smith, R. B. (1982), Synoptic observations and theory of orographically disturbed wind and pressure, *J. Atmos. Sci.*, *39*(1), 60–70, doi:10.1175/1520-0469(1982)039<0060:SOATOO>2.0.CO;2.

Smith, S. D. (1988), Coefficients for sea surface wind stress, heat flux, and wind profiles as a function of wind speed and temperature, *J. Geophys. Res.*, *93*(C12), 15,467–15,472, doi:10.1029/JC093iC12p15467.

Stoffelen, A. (1998), Toward the true near-surface wind speed: Error modeling and calibration using triple collocation, *J. Geophys. Res.*, *103*(C4), 7755–7766, doi:10.1029/97JC03180.

Swift, J. H., and K. Aagaard (1981), Seasonal transitions and water mass formation in the Iceland and Greenland seas, *Deep Sea Res., Part A*, *28*(10), 1107–1129, doi:10.1016/0198-0149(81)90050-9.

The Lab Sea Group (1998), The Labrador Sea deep convection experiment, *Bull. Am. Meteorol. Soc.*, *79*(10), 2033–2058, doi:10.1175/1520-0477(1998)079<2033:TLSDCE>2.0.CO;2.

Våge, K., R. S. Pickart, G. W. K. Moore, and M. H. Ribergaard (2008), Winter mixed layer development in the central Irminger Sea: The effect of strong, intermittent wind events, *J. Phys. Oceanogr.*, *38*(3), 541–565, doi:10.1175/2007JPO3678.1.

Våge, K., R. S. Pickart, M. A. Spall, H. Valdimarsson, S. Jónsson, D. J. Torres, S. Østerhus, and T. Eldevik (2011), Significant role of the North Icelandic Jet in the formation of Denmark Strait overflow water, *Nat. Geosci.*, *4*(10), 723–727, doi:10.1038/ngeo1234.

Våge, K., R. S. Pickart, M. A. Spall, G. W. K. Moore, H. Valdimarsson, D. J. Torres, S. Y. Erofeeva, and J. E. Ø. Nilsen (2013), Revised circulation scheme north of the Denmark Strait, *Deep Sea Res., Part I*, *79*, 20–39, doi:10.1016/j.dsr.2013.05.007.

Watson, A. J., et al. (1999), Mixing and convection in the Greenland Sea from a tracer-release experiment, *Nature*, *401*(6756), 902–904, doi:10.1038/44807.

Zeng, L., and R. A. Brown (1998), Scatterometer observations at high wind speeds, *J. Appl. Meteorol.*, *37*(11), 1412–1420, doi:10.1175/1520-0450(1998)037<1412:SOAHWS>2.0.CO;2.